Forced phase-locked states and information retrieval in a two-layer network of oscillatory neurons with directional connectivity

Victor Kazantsev
Institute of Applied Physics of RAS, 46 Uljanov street, 603950 Nizhny Novgorod, Russia
and Department of Neurodynamics and Neurobiology, Nizhny Novgorod State University, 23 Gagarin Ave., 603950 Nizhny Novgorod, Russia

Alexey Pimashkin
Department of Neurodynamics and Neurobiology, Nizhny Novgorod State University, 23 Gagarin Ave., 603950 Nizhny Novgorod, Russia
(Received 11 March 2007; published 12 September 2007)

We propose two-layer architecture of associative memory oscillatory network with directional interlayer connectivity. The network is capable to store information in the form of phase-locked (in-phase and antiphase) oscillatory patterns. The first (input) layer takes an input pattern to be recognized and their units are unidirectionally connected with all units of the second (control) layer. The connection strengths are weighted using the Hebbian rule. The output (retrieved) patterns appear as forced-phase locked states of the control layer. The conditions are found and analytically expressed for pattern retrieval in response on incoming stimulus. It is shown that the system is capable to recover patterns with a certain level of distortions or noises in their profiles. The architecture is implemented with the Kuramoto phase model and using synaptically coupled neural oscillators with spikes. It is found that the spiking model is capable to retrieve patterns using the spiking phase that translates memorized patterns into the spiking phase shifts at different time scales.

DOI: 10.1103/PhysRevE.76.031912 PACS number(s): 87.19.La, 84.35.+i, 05.45.−a, 87.18.Sn

I. INTRODUCTION

The studies of principles of information representation and its processing in the brain still remain in the cutting edge field of modern neuroscience. It is believed that information is processed by evolving self-sustained activity patterns formed by neuronal networks due to local oscillatory activity of neurons and complex architecture of synaptic connections [1]. Associative memory phenomenon represents one of the most spectacular examples illustrating how the networks can effectively memorize the information and retrieve it if an appropriate stimulus has been given [2–11].

Modeling Hopfield networks with binary states and the Hebbian rule for the connectivity has provided a fundamental insight in the problem of computation with patterns [2]. Such networks can store a set of binary patterns associated with local minima of "energy" function. For certain conditions the required pattern can be retrieved or recognized if an initial stimulus hits the attraction basin of the corresponding energy minimum. The estimated storage capacity (the number of stored patterns per unit) of an n-unit system is proportional to $1/\log n$. Based on the computational principles of Hopfield networks oscillatory models for associative memory has attracted great attention and interest in recent years [3–9]. Such interest has also been stimulated by neurophysiological findings stating that the oscillatory activity can provide the background for computational functions of the brain. Take, for instance, theta-rhythm oscillations in hippocampus, 40-Hz thalamocortical activity and information binding, 10-Hz olivocerebellar oscillations and oscillatory patterns for motor control [1]. In oscillatory network models the information can be encoded using oscillation phase or spiking phase, i.e., the time moments when action potentials or spikes are generated. Such networks are capable to "translate" a sensory input or a physiological function into dynamic patterns of oscillatory activity. Take, for example, phase cluster formation for visual scene segmentation task in network with global inhibitor [12], oscillatory patterns implementing a motor command in network with oscillatory feedback [13], and the above mentioned associative memory models.

One of the simplest mathematical models for oscillatory associative memory is based on Kuramoto's network comprising a set of weakly coupled nonlinear oscillators [14]. The dynamics of the oscillators can be reduced to the analysis of phase equations

$$\frac{d\varphi_i}{dt} = \sum_{j=1}^{N} s_{ij} \sin(\varphi_j - \varphi_i) \tag{1}$$

with coupling matrix

$$s_{ij} = \frac{1}{N} \sum_{k=1}^{K} \xi_i^k \xi_j^k \tag{2}$$

implementing the Hebbian rule. The set of K vectors ξ^k encodes binary information patterns, so that ξ_j^k takes either $+1$ or -1 values. Then, the oscillations occur with either 0 (in-phase state) or π (antiphase state) phase shifts between the network units. System (1) is a gradient system, hence its attractors are steady states associated with minima of corresponding energy function. It has been shown that the error-free information retrieval is limited by $K=2$ memorized patterns [6]. The modification of Eq. (1) generalizing the coupling function has been recently proposed extending the capacity up to the Hopfield limits [10,11]. It locates the terminal patterns exactly at the in-phase and antiphase states and improves the error-free capacity up to $2\varepsilon^2/\log n$ (ε is the

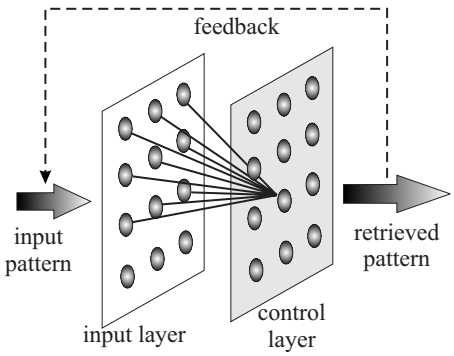

FIG. 1. A feedforward (heterogeneous) architecture of the two-layer oscillatory network for associative memory.

amplitude of the second harmonic of the coupling term expansion). However, the solutions different from the memorized pattern can become stable in the case of increasing ε.

In a more general view Kuramoto-type oscillatory networks representing a fundamental mathematical tool for understanding principles of associative memory have some difficulties to be directly related to neuronal systems. The networks are typically composed using a *bidirectional* coupling term so that units influence each other. However, synaptic architecture of neuronal connections is typically *unidirectional* comprising the presynaptic (input) and postsynaptic (output) cells. The electrical gap junctions (electrical synapses) being an appropriate treatment for the bidirectional coupling term typically have local (nearest-neighbor) architecture. Another note is that the phase description of the oscillators valid only for weak couplings yields the limitation on the real time scale of the retrieval processes to be very slow [14].

The geometry or architecture of model (1) is referred to as homogeneous in the sense that its input and output coincide. The input pattern is taken as initial conditions and the output information comes as the terminal state. In this paper we propose a two-layer feedforward (heterogeneous) architecture (Fig. 1) of the oscillatory associative memory network. It separates input and output information flows similarly to layered perceptual networks [15,16]. The units of the input layer are unidirectionally connected with the control layer with a Hebbian coupling matrix. We show that output patterns in response to appropriate stimulus appear as forced phase-locked states with perfect in-phase or antiphase values. For certain conditions the output state can perfectly reproduce or retrieve one of the memorized patterns. The storage capacity for error-free retrieval stays limited with $K=2$ memorized states as in system (1) for an arbitrary (unbiased) set of patterns. However, if the memorized patterns satisfy some conditions restricting a pattern basis or "alphabet," then the capacity can be significantly enhanced. Furthermore, we show how the two-layer associative memory can be implemented using neuronal oscillators with true spiking dynamics and excitatory or inhibitory synaptic connections. Such a network represents information using spiking times and is capable to operate at different time scales.

The paper is organized as follows. In Sec. II we give a general model description and analytically obtain the retrieval conditions using Kuramoto phase oscillators. In Sec. III we show how forced phase-locking spikes in the two-layer network composed of neural oscillators [17] can implement the associative memory using the excitatory and inhibitory synaptic connections and spike phase encoding. The Conclusion, Sec. IV, contains a brief discussion of the results.

II. TWO-LAYER PHASE OSCILLATORY NETWORK MODEL

The dynamics of the two-layer oscillatory network shown in Fig. 1 is given by the following phase equations:

$$\frac{d\varphi_i}{dt} = \sum_{j=1}^{N} s_{ij} \sin(\varphi_j^0 - \varphi_i),$$

$$\cos \varphi_j^0 = \xi_j^0 = \text{const},$$

$$\sin \varphi_j^0 = 0. \tag{3}$$

Variables φ_j describe the evolution of the control layer units and φ_j^0 are constant input phases defined by the input information pattern ξ_j^0 fixed with $+1$ and -1 values. The coupling coefficient s_{ij} is taken according to the Hebbian rule (2). Note that the oscillators in the second layer are uncoupled with each other and evolve under a constant input stimulus.

A. Retrieval dynamics

Let us consider the retrieval dynamics of the two-layer model (3). Since the input phases φ_j^0 are fixed with 0 or π values the fixed points of the first equation in Eq. (3) are given by

$$\sin \varphi_i \sum_{j=1}^{N} s_{ij} \xi_j^0 = 0. \tag{4}$$

Let us assume that the coefficients $\Sigma_{j=1}^{N} s_{ij} \xi_j^0$ are not equal to zero.[1] Then, the fixed points of the control layer are located exactly at 0 or π states. Similarly to Eq. (1), system (3) is a gradient system and its stable fixed points correspond to the minima of the energy (Lyapunov) function. Since the oscillators in the control layer are independent for each unit the function is expressed as

$$\Pi(\varphi_i) = -\sum_{j=1}^{N} s_{ij} \cos(\varphi_j^0 - \varphi_i), \tag{5}$$

$$\varphi_i = -\frac{d\Pi(\varphi_i)}{d\varphi_i}.$$

In other words the Jacobian defining the pattern stability of the fixed points in N-dimensional space has only diagonal terms.

[1]Zero values of the coefficients correspond to a neutral stability mode. It can be excluded by a small structural perturbation of the right-hand side function [6].

Let us now analyze the shape of energy functions when an unbiased set ξ^k $(k=1,2,\ldots,K)$ of information patterns is memorized using the Hebbian rule (2). It follows from Eq. (5) that

$$\Pi(\varphi_i) = -\frac{1}{N}\sum_{j=1}^{N}\sum_{k=1}^{K}\xi_i^k\xi_j^k\cos(\varphi_j^0-\varphi_i)$$

$$= -\frac{1}{N}\sum_{j=1}^{N}\sum_{k=1}^{K}\xi_i^k\xi_j^k(\cos\varphi_j^0\cos\varphi_i+\sin\varphi_j^0\sin\varphi_i).$$

Using Eq. (3) we obtain

$$\Pi(\varphi_i) = -\cos\varphi_i\sum_{k=1}^{K}\xi_i^k\frac{1}{N}\sum_{j=1}^{N}\xi_j^k\xi_j^0. \tag{6}$$

Thus the energy function for each unit has only one minimum corresponding to the stability of either 0 or π states depending on the sign of the sum in Eq. (6). Note that the quantity

$$m_k^0 = \frac{1}{2}\left(\frac{1}{N}\sum_{j=1}^{N}\xi_j^k\xi_j^0+1\right)$$

characterizes the overlap between the initial pattern and the kst pattern from the memorized set. It takes +1 value if the patterns are absolutely identical and 0 if they are completely different.

B. Capacity characteristics

Let us now specify that we would like to retrieve one of the patterns, ξ^r, from the memorized set. Let M be the number of components of vector ξ^0 with +1 values. Then, for units from this group Eq. (6) takes the form

$$\Pi(\varphi_i) = -\cos\varphi_i\sum_{k=1}^{K}\xi_i^k\frac{1}{N}\left[\sum_{j=1}^{M}\xi_j^k-\sum_{j=M}^{N}\xi_j^k\right]$$

$$= -\cos\varphi_i\sum_{k=1}^{K}\xi_i^k\frac{1}{N}[N-2P_k],$$

where $P_k=N(1-m_k^0)$ is the measure of discrepancy between the kst pattern and the input pattern. Then, the condition for error-free retrieval of the pattern ξ^r can be written as

$$N-2P_r > -\sum_{\substack{k=1\\k\neq r}}^{K}\xi_i^r\xi_i^k[N-2P_k], \quad \forall\ i=1,2,\ldots,N. \tag{7}$$

Let the input pattern be close to ξ^r so that $P_r=\delta\ll N$. Furthermore, a sufficient condition for error-free retrieval is estimated from inequalities (7) as

$$N-2\delta > (K-1)|N-2(Q-\delta)|, \tag{8}$$

where $Q=\min P_k$ is the minimum discrepancy between the patterns in the memorized set. It follows from Eq. (8) that the information capacity of the model (3) is restricted by

$$K < 1+\frac{N}{|N-2Q|}. \tag{9}$$

For an unbiased set of patterns the capacity stays limited as in the classical oscillatory network (1) with the $K=2$ memorized patterns. However, if the set of patterns is selected according to some basis or "alphabet" with $Q\to N/2$, then according to Eq. (9) the capacity can be significantly increased. In fact, it is an expression of the general rule for Hopfield networks that distinguishable patterns should be quite distant from each other.

Nevertheless, if Eq. (9) is satisfied the system can discriminate close patterns. Let $K=2$ similar patterns with just one different pixel at $i=i^*$ $(\xi_{i^*}^1=-\xi_{i^*}^2, \xi_j^1=\xi_j^2, j\neq i)$ be stored in the memory. If the input has discrepancy $P_1=P$ with the first pattern and contains the same pixel at $i=i^*$ $(\xi_{i^*}^0=-\xi_{i^*}^1)$ then its discrepancy with the second pattern will be $P_2=P+1$. In this case the inequalities (7) for error-free retrieval of the first pattern will be written as

$$N-2P > -\xi_{i^*}^1(-\xi_{i^*}^1)[N-2(P+1)] = N-2P-2,\ i=i^*,$$

$$N-2P > -\xi_i^1\xi_i^1[N-2(P+1)] = -[N-2P]+2, \quad i\neq i^*.$$

They ensure the correct retrieval of the first pattern for $P<(N-1)/2$.[2] Otherwise, a "mirror image" of the pattern will appear in the output.

Another feature of the two-layer model (3) is that it can distinguish mirror images. Let us assume that two mirror patterns have been memorized. In this case $\xi_i^r\xi_i^k<0$ and the inequalities (7) become $N>2P_r$ which ensures the correct retrieval for small initial discrepancy. This is the result of the two-layer organization of the network breaking the symmetry in Eq. (1) relative to the phase difference between the oscillators in the control layer.

Note that the profile of energy function (6) for model (3) is defined not only by the memorized pattern set but also depends on the initial pattern or on the initial overlap. It is quite different from the homogeneous case of Eqs. (1) where the memory structure is represented by a certain number of local minima attracting the initial conditions from their basins. The energy function (6) has the only one minimum globally asymptotically stable in the N-dimensional phase space and its configuration due to the stimulus defines the memory function. The retrieval dynamics is independent of the initial conditions in the control layer.

C. Perfect and imperfect retrieval, recovery of distorted information

It follows from Eq. (6) that the terminal pattern in Eqs. (3) can be expressed as

[2]Note that if there is an even number of different pixels between the patterns the retrieval of them may lead to a neutral stability mode for some set of input patterns. Such input patterns cannot be discriminated in the model.

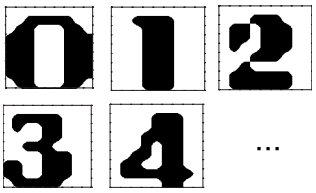

FIG. 2. A set of information patterns in the form of 10×10 binary images of digits memorized in the oscillatory network.

$$\xi_i^{out} = 2\Theta\left(\sum_{k=1}^{K} \xi_i^k (2m_k^0 - 1)\right) - 1,$$

$$m_k^{out} = \frac{1}{2}\left(\frac{1}{N}\sum_{i=1}^{N} \xi_i^{out}\xi_i^k + 1\right), \tag{10}$$

where m_k^{out} is the overlap between the retrieved pattern and the kst pattern from the memory, Θ is the Heaviside function.

Let us consider a set of patterns loaded into the network using Eq. (2). We arrange the units in a two-dimensional $(\sqrt{N}\times\sqrt{N})$ square lattice and take the pattern set as binary images of digits {**0**, **1**, **2**,…} (Fig. 2) [9]. To illustrate our theoretical predictions we focus on the concrete pattern "alphabet" characterized by the interpattern overlaps that is a principle characteristic for the retrieval performance. The input patterns are taken distorted with noise according to the formula

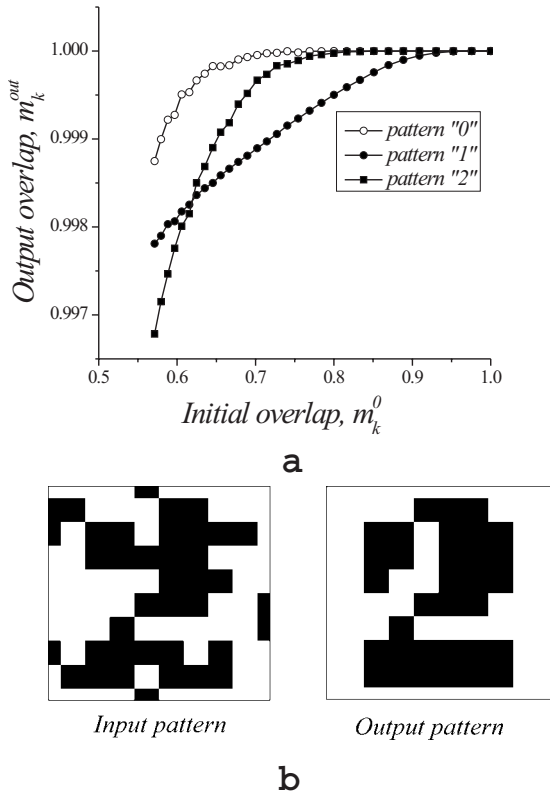

FIG. 3. (a). Retrieved pattern overlaps vs initial overlaps for the case of perfect retrieval with $K=3$ patterns memorized, $Q=0.25N$ in Eq. (9). Overlap values are averaged among 10^6 trials of input patterns distorted according to formula (11). (b) Retrieving the digit 2 from a distorted initial stimulus. White and black colors correspond to in-phase and antiphase states, respectively.

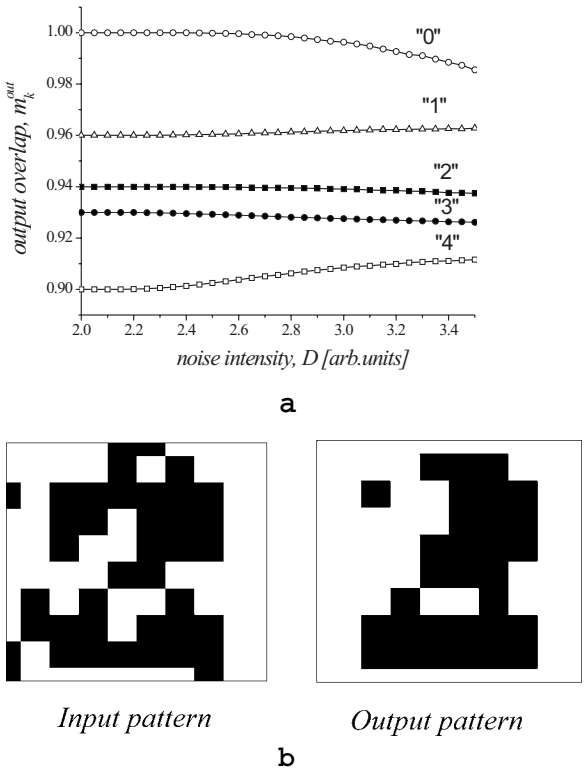

FIG. 4. Imperfect retrieval for $K=5$ memorized digits. (a) The dependence of the averaged overlaps on noise intensity. Images are retrieved with different quality. Some of them can be improved by the initial distortions. (b) Imperfect retrieval of the digit 2. White and black colors correspond to in-phase and antiphase states, respectively.

$$\xi_i^0 = 2\Theta(\xi_i^k + D\eta_i) - 1, \tag{11}$$

where η_i are uncorrelated random values uniformly distributed within the interval $[-1,1]$. Figure 3(a) illustrates output overlap (10) vs initial overlap for the set of $K=3$ patterns satisfying condition (9). It appears that all three patterns can be perfectly retrieved (or recovered) if the initial stimulus has less than about 10% distortions with the desired one. The example of the recovered pattern **2** is shown in Fig. 3(b).

If condition (9) is not satisfied, oscillatory model (3) exhibits a certain level of distortions in the profile of the output pattern. In this case it is still capable to recognize or classify the incoming information by minimizing the discrepancy (or maximizing the overlap) between the retrieved pattern and the one from the memorized set. To illustrate how the retrieval process depends on the initial distortion level we plot in Fig. 4(a) the output overlap vs parameter D explicitly for $K=5$ memorized patterns. It appears that different patterns from the memorized set are processed with different quality. For example, the first pattern (digit **0**) is perfectly retrieved for sufficiently small initial distortions. Note that the output overlap for some of them increases with increasing initial

distortions indicating that perturbations can improve the retrieving dynamics. In spite of the imperfections the cores of the output patterns can be recognized as one of the memorized images [Fig. 4(b)].

We also note that the directional architecture of the model (3) can be added with appropriate feedback to improve the retrieving quality. Using such feedback the terminal pattern can be mapped back to the first layer and can be recurrently taken as the input pattern. The iterations may be stopped when the overlap reaches its maximal value. For example, in the case of three images memorized (Fig. 3) one additional iteration of the pattern would be sufficient for perfect retrieval [Fig. 3(a)].

III. SPIKING OSCILLATORY NETWORK

The principle dynamical mechanism leading to the associative memory function in the oscillatory network (3) is the interlayer phase locking due to the directional connectivity. Depending on the sign of the total input sum in Eq. (3) each unit of the control layer exhibits either the in-phase-locked or the antiphase-locked synchronous mode globally stable in the phase space. We now illustrate how the associative memory based on the force phase-locking effect can be implemented in an oscillatory network of spiking neurons with excitatory or inhibitory synaptic architecture.

A. Model description

We consider the two-layer feedforward architecture shown in Fig. 1 composed of two-variable spiking oscillators [17] often used for modeling interneuron synchronization [19]. We take the equations for a unit of the control layer in the form

$$\begin{cases} \tau_m \dfrac{dV_i}{dt} = -I_{fast}(V_i) - I_{syn}(V_i, V_k^0) - W; \\ \tau_w(V_i)\dfrac{dW_i}{dt} = W_\infty(V_i) - W_i. \end{cases} \tag{12}$$

The first equation describes a membrane current balance equation with V_i and V_k^0 being the membrane potential deviations of the cell and a presynaptic cell from the input layer. The instantaneous current $I_{fast}(V)=-V+\tanh(g_{fast}V)$ combines the leak current and fast V-dependent inward current. A slow variable W represents the slow recovery current, with voltage dependent activation function $W_\infty(V)=g_{slow}V$, $\tau_w(V)=[\tau_2+(\tau_1-\tau_2)/(1+1/\exp(V/k_\tau)]$ is the voltage dependent time constant of the slow current. It approaches $\tau_1 \gg \tau_m$ during the active phase ($V>0$, a slowly activating outward current) and $\tau_2 \gg \tau_m$ during the silent phase ($V<0$, a slowly activating inward current). Synaptic transmission is instantaneous, with a synaptic current given by $I_{syn}=g_{syn}S_\infty(V_k^0)(V_i-V_{syn})$, where g_{syn} is the maximal synaptic conductance, V_{syn} is the synaptic reversal potential, and the sigmoid function $S_\infty(V_k^0)=1/\{1+1/\exp[(V_k^0-\theta_{syn})/k_{syn}]\}$. Depending on values of V_{syn} the synaptic transmission can be referred to as excitatory ($V_{syn}>0$) or inhibitory ($V_{syn}<0$).

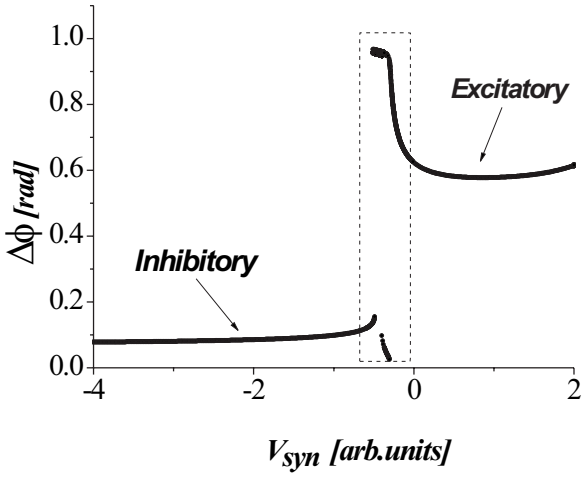

FIG. 5. Spiking phase shift dependence on synaptic reversal potential for two synaptically coupled neural oscillators [19]. The dashed rectangle shows the "uncertainty" region where the oscillations cannot be set in-phase or antiphase. Parameter values: $\tau_1=5$, $\tau_2=50$, $k_\tau=0.05$, $\tau_m=0.16$, $g_{fast}=2$, $g_{slow}=2$, $I_{app}=0.6$, $g_{syn}=0.1$, $\theta_{syn}=0.0$, $k_{syn}=0.2$.

B. Force phase-locking modes due to synaptic coupling

Let us consider the dynamics of two cells (12) with unidirectional synaptic connection. Possible dynamical modes and locking effects by the synaptic coupling were analyzed in detail previously [18–20]. Here we are interested in stabilizing the in-phase and antiphase spiking modes for the unidirectional connection. We defined the spiking phase using time the difference between postsynaptic and presynaptic spikes:

$$\varphi(n) = \frac{t_{post}(n) - t_{pre}(n)}{T}, \quad n = 1,2, \ldots, \tag{13}$$

where t_{post} and t_{pre} are the time moments of a postsynaptic spike and preceding presynaptic spike, respectively, n is a digital number of the spikes in the sequence, T is the oscillation period. Using the procedure described in [21] the spiking phase map has been constructed for model (12). The map defines the attractors and their basins for the phase variable (13). The results are illustrated using the one-parameter bifurcation diagram shown in Fig. 5. The points of the graph indicate the fixed point attractors (stable values of the spiking phase) for different values of V_{syn}. It appears that for inhibitory ($V_{syn}<0$) and for excitatory ($V_{syn}>0$) couplings there are two regions corresponding to globally stable almost in-phase- and almost antiphase-locking modes, respectively. We further use this property to construct the synaptic architecture for associative memory.

C. Synaptic architecture for associative memory

To implement the two-layer architecture for associative memory the total synaptic current for an oscillator taken from the control layer is given by the sum of synaptic currents from all input layer cells:

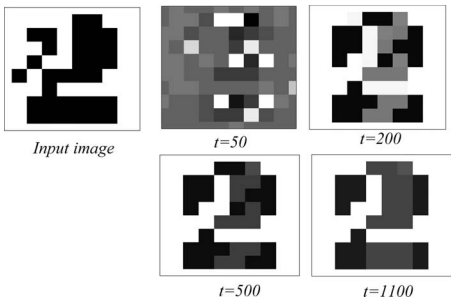

FIG. 6. Information retrieval in the two-layer network of neural oscillators. The sequence of snapshots illustrating spiking phase distribution in the control layer. Gray scale color grade corresponds to the phase shifts distributed from white (in-phase) to black (antiphase). Unit parameters are the same as in Fig. 5, $a=-2.5$, $b=-1.5$.

$$I_{syn}(V_i) = \frac{1}{N}\sum_{j=1}^{N} \frac{g_{syn}(V_i - V_{syn,ij})}{1+\exp[(-V_j^0 - \theta_{syn})/k_{syn}]}, \qquad (14)$$

where V_j^0 is the presynaptic potential of the jst cell from the input layer, $V_{syn,ij}$ are the reversal potentials of the interlayer synaptic contacts. To implement the associative memory we encode the distribution of the synapses between excitatory and inhibitory according to the values of the Hebbian matrix s_{ij}, $V_{syn,ij}=V^s(s_{ij})$, so that positive and negative elements of s_{ij} provide the in-phase- and the antiphase-locking modes for the inhibitory and excitatory synapses, respectively (Fig. 5). We take $V^s(s_{ij})$ in a simple linear form, $V^s(x)=ax+b$. The coefficients $a=-5/2$ and $b=-3/2$ are chosen to set particular values of the reversal potential, $V_{syn,ij}=-4$ for $\xi_i\xi_j=+1$ (inhibitory synapse$\rightarrow$in-phase mode) and $V_{syn,ij}=+1$ for $\xi_i\xi_j=-1$ (excitatory synapse$\rightarrow$antiphase mode).

Let us assume that the input layer contains a binary information pattern encoded by using the spiking phase (13). It is easy to do, for example, by stimulating each unit of the first layer by the same periodic stimulus with appropriately distributed values of the reversal potential, i.e., $V_{syn,j}^0=-4$ for $\xi_i^0=+1$ and $V_{syn,j}^0=+1$ for $\xi_i^0=-1$. Such a periodic stimulus can be taken from an isolated base oscillator described by Eq. (12). Its spiking times can be also used to count phase shift distributions for the layers according to Eq. (13). Since each unit of the first layer gets the same synaptic input it becomes force phase locked relative to the base oscillator with either in-phase or antiphase spiking [Fig. 6(a)]. Then, for the control layer we can split the synaptic current given by Eq. (14) on two terms as follows:

$$I_{syn}(V_i) = \frac{g_{syn}\left(\frac{M}{N}V_i - a\sum_{k=1}^{K}\xi_i^k\frac{1}{N}\sum_{j=1}^{M}\xi_j^k - b\right)}{1+\exp[(-V^{0+}-\theta_{syn})/k_{syn}]} + \frac{g_{syn}\left([(N-M)/N]V_i - a\sum_{k=1}^{K}\xi_i^k\frac{1}{N}\sum_{j=M}^{N}\xi_j^k - b\right)}{1+\exp[(-V^{0-}-\theta_{syn})/k_{syn}]}. \qquad (15)$$

The first term is driven by the synchronized signal $V^{0+}(t)$ corresponding to $\xi_i^0=+1$ pixels of the input image. The second term corresponds to $\xi_i^0=-1$ pixels and is driven by $V^{0-}(t)$ that appears almost antiphase relative to $V^{0+}(t)$. The two terms tend to synchronize the control layer units with either in-phase or antiphase spiking depending on the values of the reversal potentials (Fig. 5). Then, to estimate the terminal locking mode we can merge the two terms into one driven by the synchronized signal as follows

$$I_{syn}(V_i) \approx \frac{g_{syn}\left[V_i - a\sum_{k=1}^{K}\xi_i^k\frac{1}{N}\left(\sum_{j=1}^{M}\xi_j^k - \sum_{j=M}^{N}\xi_j^k\right) - b\right]}{1+\exp(-V^{0+}-\theta_{syn}/k_{syn})}, \qquad (16)$$

with the opposite sign of the sum encoding the reversal potential parameter. Thus we obtain that the phase-locked mode of the control layer units is defined by the sum

$$\sum_{k=1}^{K}\xi_i^k\frac{1}{N}\left(\sum_{j=1}^{M}\xi_j^k - \sum_{j=M}^{N}\xi_j^k\right).$$

If we assume that positive and negative signs of the sum provide perfect antiphase and in-phase modes we find that the retrieved pattern configuration is defined by formula (7) obtained for the phase model. Accordingly, if the pattern set satisfies the condition (9) ($K=3$, Fig. 3) for error-free retrieval the system performance relative to each pattern is determined by the curves shown in Fig. 3(a). However, the phase diagram of Fig. 5 defining the locking modes depending on V_{syn} has an "uncertainty" region (marked by the dashed rectangle). In this region the in-phase and antiphase modes cannot be distinguished. There is also bistability when the phase values depend on initial conditions. The uncertainty interval results in the appearance of *dynamical* distortions of the retrieved pattern (in addition to the distortions due to the limited capacity). These distortions (of order of 1–3 %) are independent of the initial overlap values and are defined only by the imperfection of the force phase-locking modes in the uncertainty region. Note, however, that the uncertainty can be excluded by a nonlinear dependence of the synaptic reversal potentials on the elements of the connection matrix, $V^s(s_{ij})$. For instance, it can be a Heaviside-like function that maps the matrix values out of this region.

Figure 6 illustrates the sequence of retrieved phase images obtained for the same conditions for the memorized pattern set as in Fig. 3. Time evolution of phase variable (13) and membrane potentials of the units are shown in Fig. 7. Since the phase response values (Fig. 5) of the synaptic transmission does not provide the exact in-phase- and antiphase-locking modes the retrieved phases in model (12) and (14) do not perfectly coincide [Figs. 7(a) and 7(c)]. However, they apparently form two separate groups or clusters corresponding to a binary distribution. Note also that interunit spiking time lags inside the in-phase and antiphase clusters appear to be distributed within a narrow band [Fig. 7(c)]. Moreover, at the time scale of this band the signals sequentially display the distributions corresponding to other information patterns memorized in the system (Fig. 8). It is explained by fact that the regions of in-phase and antiphase

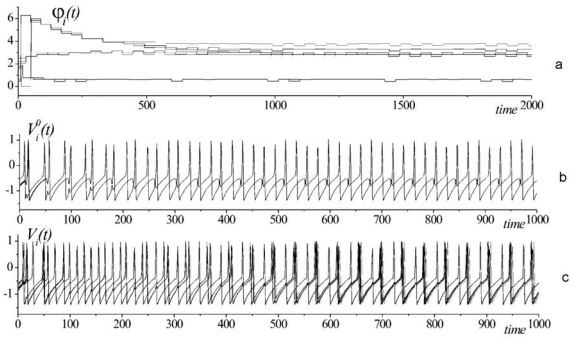

FIG. 7. (a) Time evolution of the spiking phase (13) of the control layer units forming phase clusters. (b) Time evolution of membrane potential of the input layer units forming two groups with perfect in-phase and antiphase spiking. (c) Time evolution of control layer units. The spikes within the antiphase cluster are distributed with certain time lags associated with the distortions of the retrieved image. Parameters are the same as in Fig. 6.

locking (Fig. 5) are not perfectly flat but have a finite slope. Then, the values of s_{ij} for each unit encoding the composite reversal potential according to formula (16) result in slightly different resulting phases between units. Since these differences are produced by different values of the Hebbian matrix that, indeed, contains the information about all memorized patterns, the spiking model (12) and (14) transforms this information into different phase lags between spikes. A similar effect of visual scene segmentation was achieved in the spiking model with global inhibitor [12] where the set of objects was represented by groups of synchronized oscillators with definite phase shift. Accordingly, in our model of associative memory we can treat the phase lags between the memorized information patterns ("segments of the memory") as a possible mechanism of memory segmentation.

IV. CONCLUSION

We have proposed a two-layer oscillatory network for associative memory capable to store a set of binary patterns and retrieve one of them if an appropriate stimulus is applied. The model has a feedforward (heterogeneous) architecture with the input layer containing a stimulus and the control (output) layer that retrieves a desired pattern. The information is encoded using stable in-phase and antiphase locked modes corresponding to binary patterns. The network has a directional interlayer connectivity, i.e., the units of the control layers are stimulated by a composite (converged) signal from all input layer units. We use the standard Hebbian rule to define the strengths of this stimulation. The oscillatory units have been modeled by phase oscillators representing a reduced (phase) description of the Kuramoto network of weakly coupled oscillators. The dynamics of the control layer network is defined by the force phase-locking effect that provides the exact in-phase or antiphase fixed point attractors. The retrieved pattern configuration is given by the energy (Lyapunov) function. In contrast with homogeneous

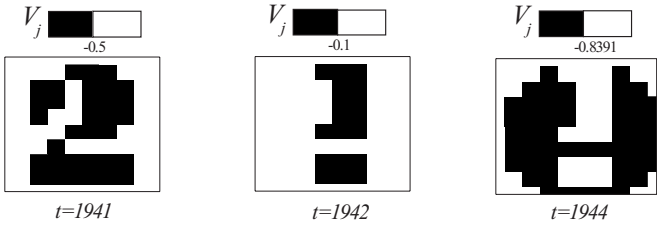

FIG. 8. Sequence of snapshots of the V_j variables taken within time distributed antiphase cluster. The system sequentially recalls the two memorized images (0 and 1) other than the retrieved one at the very short time scale.

oscillatory networks it has just one globally stable minimum attracting all initial conditions. Its spatial configuration is defined by the stimulus pattern. Therefore if no stimulus is applied then the network units evolve independently preserving an earlier given pattern or without any configuration. Indeed, the system has no "internal associations" like homogeneous networks that internally contain the set of local minima corresponding to information patterns. In this sense the term "associative memory" seems to be not quite precise to define the phenomenon. It is more a stimulus-induced associative function when the stimulus forces the system to recall and retrieve the required pattern. Although the model does not give quite significant improvements in its error-free capacity it has obvious advantages in its simplicity and dynamical robustness. Note that the retrieved function does not depend on the initial conditions hence the system can be easily switched from one pattern to another.

Another advantage concerns the possibility to implement this solution using spiking neuronal oscillators. The spikes and spiking phases are believed to be the main information carriers in the nervous system. We have illustrated this possibility using simple neuronal oscillators with spikes. Due to the directional connectivity the interlayer interaction has been organized with excitatory and inhibitory synaptic currents. The effect of force phase locking yields the associative information retrieval using relative spiking phase or phase shifts. Moreover, in contrast with phase oscillators having time averaged dynamics, the spiking units can provide the segmentation of the memorized set at a shorter time scale. This can be also viewed as the translation of information encoded by synaptic architecture into the true dynamical representation using spikes as the information carriers.

ACKNOWLEDGMENTS

This work was supported by the Russian Foundation for Basic Research (Grants No. 05-02-17441, No. 06-02-16137, No. 05-02-19185), by the grant of the President of Russian Federation (Grant No. MD-4602.2007.2), by the grant for Leading Scientific Schools of the Russian Federation (No. 7309.2006.2), and by the CRDF Foundation (REC-006, Grant No. Y2-P-06-04). We also acknowledge the anonymous referees whose valuable comments have helped to improve the paper.

[1] R. Llinas, *I of the Vortex: From Neurons to Self* (MIT Press, Cambridge, MA, 2001).
[2] J. Hopfield, Proc. Natl. Acad. Sci. U.S.A. **79**, 2554 (1982).
[3] L. F. Abott, J. Phys. A **23**, 3835 (1990).
[4] T. Aoyagi, Phys. Rev. Lett. **74**, 4075 (1995).
[5] T. Aonishi, K. Kurata, and M. Okada, Phys. Rev. Lett. **82**, 2800 (1999).
[6] T. Aonishi, Phys. Rev. E **58**, 4865 (1998).
[7] T. Aoyagi, Neural Comput. **10**, 1527 (1998).
[8] M. Yoshioka and M. Shiino, Phys. Rev. E **58**, 3628 (1998).
[9] F. C. Hoppensteadt and E. M. Izhikevich, Phys. Rev. Lett. **82**, 2983 (1999); Phys. Rev. E **62**, 4010 (2000).
[10] T. Nishikawa, Y.-C. Lai, and F. C. Hoppensteadt, Phys. Rev. Lett. **92**, 108101 (2004).
[11] T. Nishikawa, F. C. Hoppensteadt, and Y.-C. Lai, Physica D **197**, 134 (2004).
[12] D. Terman and D. Wang, Physica D **81**, 148 (1995).
[13] V. B. Kazantsev, V. I. Nekorkin, V. I. Makarenko, and R. Llinas, Proc. Natl. Acad. Sci. U.S.A. **100**, 13064 (2003).
[14] Y. Kuramoto *Chemical Oscillations, Waves, and Turbulence* (Springer-Verlag, Berlin, 1984).
[15] R. Linsker, Computer **21**, 105 (1988).
[16] T. L. H. Watkin, A. Rau, and M. Biehl, Rev. Mod. Phys. **65**, 499 (1993).
[17] P. Rowat and A. I. Selverston, J. Neurophysiol. **70**, 1030 (1993).
[18] J. Rubin and D. Terman, J. Math. Biol. **41**, 513 (2000).
[19] T. Bem and J. Rinzel, J. Neurophysiol. **91**, 693 (2004).
[20] K. Tsumoto, T. Yoshinaga, K. Aihara, and H. Kawakami, Int. J. Bifurcation Chaos Appl. Sci. Eng. **13**, 653 (2003).
[21] V. B. Kazantsev, V. I. Nekorkin, S. Binczak, S. Jacquir, and J.-M. Bilbalt, Chaos **15**, 023103 (2005).